Electronic states of ultrathin InAs/InP (001) quantum wells: A tight-binding study of the effects of band offset, strain, and intermixing

N. Shtinkov,* P. Desjardins, and R. A. Masut
Département de Génie Physique and Groupe de Recherche en Physique et Technologie des Couches Minces (GCM), École Polytechnique de Montréal, C.P. 6079, Succursale "Centre-Ville," Montréal QC, H3C 3A7, Canada
(Received 8 April 2002; revised manuscript received 15 July 2002; published 1 November 2002)

We investigate theoretically the electronic structure of strained ultrathin InAs/InP (001) quantum wells (QWs), using the semiempirical $sp^3d^5s^*$ nearest-neighbors tight-binding model, the virtual crystal approximation, and the surface Green's function matching method. The energies of the bound states and the optical transitions are calculated for QW widths from 1 to 4 monolayers and for valence band offsets varying from 0.2 to 0.9 eV. The dependence of the transition energies on strain is investigated. The intermixing effects are studied for (i) graded interfaces with a diffusion concentration profile and (ii) $InAs_xP_{1-x}$/InP QWs of varying composition with abrupt interfaces. The effect of strain on the transition energies is found to be small for thin wells, whereas the effect of intermixing is significant and cannot be neglected. Comparing the results with experimental data, we conclude that the electronic structure of ultrathin InAs/InP (001) QWs cannot be accurately described within the simple model of a rectangular QW. The effect of intermixing however is sufficient to explain the experimental results within a reasonable range of band offsets and structure parameters.

DOI: 10.1103/PhysRevB.66.195303 PACS number(s): 73.21.Fg, 78.67.De

I. INTRODUCTION

Ultrathin InAs/InP quantum wells (QWs) have recently received considerable attention since, besides their potential applications in optoelectronic devices,[1] they provide an interesting simple materials system for fundamental studies.[2–5] The electronic states in ultrathin QWs are still not well understood. The majority of works rely on the envelope function approximation (EFA) in order to describe theoretically the electronic structure. The predictions of the EFA models however are highly questionable in the case of ultrathin QWs, as has been shown by recent tight-binding (TB) calculations.[6–8] The experimental data for ultrathin InAs/InP QWs, in particular, show significant discrepancies with the results from EFA calculations.[2,3] A recent TB calculation[5] also failed to explain the experimentally observed transition energies in these systems.

The discrepancies between theory and experiment are usually attributed to monolayer fluctuations in the QW width, leading to additional lateral confinement of excitons and therefore changing the transition energies, or to the possible failure of macroscopic elasticity theory to properly predict the interatomic spacing in layers with thicknesses in the monolayer range. However, there are a number of questionable assumptions usually made in theoretical calculations, which may lead to deviations in the obtained results. One of the most important approximations is to assume abrupt interfaces, where the transition between the well and the barrier material occurs within one monolayer (ML). Real interfaces, however, are in most cases nonabrupt due to grading and interface roughness. It has been shown that a very small amount of interface grading can alter significantly the transition energies and can change the electronic properties of lattice-matched systems.[9–12] The effect of interface grading on the electronic states of strained-layer semiconductor heterostructures is still underinvestigated. There is experimental evidence that significant intermixing may occur at InAs/InP heterojunctions (see, e.g., Refs. 13 and 14). Its impact on the electronic states, however, has been theoretically studied only in intentionally annealed structures.[15] For strained heterojunctions the effect of grading is twofold: the change of the concentration profile leads to a change of the potential of the QW in the same way as in lattice-matched systems, but it also leads to a change of the strain field in the growth direction due to the smooth transition between the two materials. It can be expected that these effects will be more pronounced in ultrathin QWs, because thinner wells are more sensitive to changes of the interface potential. Thus, taking into account the interface grading should provide a more adequate model of the electronic structure of such systems.

Another possible effect of intermixing is to have a certain nonzero concentration of the barrier material in the well layer. This would lead to a QW in which the total amount of the well material is not equal to an integer number of monolayers. To the best of our knowledge, this possibility has not been investigated with TB methods until now (in previous studies on interdiffusion[10–12] the amount of the well material is kept constant and equal to that of a perfect rectangular QW). The effect of strain on the electronic states also has to be considered in order to take into account the possible strain relaxation in such structures, and also to assess the effect of the possible deviations in the calculated energies due to the use of the macroscopic elasticity theory.

In this work we present tight-binding calculations of the electronic states in ultrathin InAs/InP (001) QWs. We start in Sec. II with a brief outline of the theoretical models used for the calculations. In Sec. III we investigate systematically the effect of the band offset, strain, and intermixing on the transition energies of QWs with thicknesses from 1 to 4 ML. The intermixing effects are studied by considering (i) graded interfaces with a diffusion concentration profile and (ii)

TABLE I. Band gaps and effective masses at the Γ point for unstrained bulk InAs and InP, and for InAs biaxially compressed in the (001) plane to the lattice constant of InP. The values in the columns (sp^3s^*) and ($sp^3d^5s^*$) are calculated using the tight-binding models of Refs. 18 and 19, respectively. The values from Ref. 16 are based on a critical review of the available experimental and theoretical data.

	InP			InAs			Strained InAs		
Parameter	sp^3s^*	$sp^3d^5s^*$	Ref. 16	sp^3s^*	$sp^3d^5s^*$	Ref. 16	Parameter	sp^3s^*	$sp^3d^5s^*$
E_g, eV	1.410	1.424	1.424	0.430	0.418	0.418	E_g(HH), eV	0.511	0.443
							E_g(LH), eV	0.670	0.600
m_e^*/m_0	0.128	0.074	0.080	0.038	0.024	0.026	$m_{e\|\|}^*/m_0$	0.049	0.025
							$m_{e\perp}^*/m_0$	0.063	0.039
m_{hh}^*/m_0	0.600	0.387	0.532	0.436	0.318	0.333	$m_{hh\|\|}^*/m_0$	0.071	0.041
							$m_{hh\perp}^*/m_0$	0.041	0.030
m_{lh}^*/m_0	0.133	0.099	0.121	0.043	0.029	0.027	$m_{lh\|\|}^*/m_0$	0.109	0.062
							$m_{lh\perp}^*/m_0$	0.120	0.099

$InAs_xP_{1-x}$/InP QWs of varying composition with perfectly abrupt interfaces. The results are compared with experimental data. The final discussion and conclusions are presented in Sec. IV.

II. THEORETICAL DETAILS

We start by choosing an appropriate TB model for performing the calculations. We consider two candidates: the nearest-neighbors sp^3s^* model of Vogl *et al.*[17] with parameters modified in order to include the spin–orbit coupling,[18] and the newer $sp^3d^5s^*$ model of Jancu *et al.*[19] (in the original work the spin–orbit coupling is taken into account). In order to compare the two models, we have calculated the band edge energies and the effective masses at the Γ point of the Brillouin zone in bulk unstrained InP and InAs. The results are shown in Table I. The data from a recent reference work[16] are also shown in the table. The latter are derived from a critical review of all the available experimental and theoretical data on the investigated compounds.

It is seen that there are large discrepancies between the results obtained using the older sp^3s^* model and the reference data for both the band gaps and the effective masses, except for the InP hole masses. This is a consequence of the fact that the sp^3s^* parameters given in Ref. 18 are based on outdated band structure data, and is also due to the intrinsic deficiencies of the nearest-neighbors sp^3s^* TB scheme.[20] In contrast, the $sp^3d^5s^*$ model gives exact results for the band edge energies. The effective masses obtained by the $sp^3d^5s^*$ model also are in good agreement (within 8%) with the experimental data except for the InP valence band effective masses, where the differences are 28% for the heavy hole mass and 18% for the light-hole mass. Since the ground states energies depend mainly on the band edge energies and on the effective masses *in the well*, it is evident that, at least for our purposes, the description of the electronic structure obtained by the $sp^3d^5s^*$ TB model is much better than the one obtained by the commonly used sp^3s^* model. Therefore we adopt the $sp^3d^5s^*$ model for our calculations.

The strain is incorporated in the TB Hamiltonian as usual, scaling the two-center integrals $ij\kappa$ with the bond length using a modified Harrison's rule[21]

$$ij\kappa(d)=\left(\frac{d_0}{d}\right)^{\nu_{ij\kappa}} ij\kappa(d_0), \tag{1}$$

where d (d_0) is the strained (unstrained) interatomic distance. For the exponents $\nu_{ij\kappa}$ we use the values of Ref. 18 (sp^3s^*) and Ref. 19 ($sp^3d^5s^*$), which are obtained by fitting the bulk deformation potentials. The strain-induced crystal-field splitting of the on-site *d*-orbital energies is also taken into account.[19] The interplane distances in the direction perpendicular to the interfaces are calculated using the macroscopic elasticity theory, with bulk lattice constants and elasticity moduli of InAs and InP taken from Ref. 16. The calculated band gaps and the effective masses of InAs, biaxially compressed in the (001) plane to the bulk lattice constant of InP are also shown in Table I. The calculated conduction- and valence-band dispersion curves of the bulk compounds in the ⟨100⟩ and ⟨111⟩ directions are shown in Fig. 1.

The material parameters at the interfaces and in the $InAs_xP_{1-x}$ alloy are calculated using the virtual-crystal bulk parameters in the following manner: for the parameters of a cation (In) layer the average concentration of As in the two adjacent anion (As_xP_{1-x}) layers are taken; for the parameters of an anion layer the concentration of As in this layer is used; and for the parameters of the interaction between a cation and an anion layer the concentration of As in the anion layer is used. This approach is widely used in tight-binding heterostructure calculations and ensures the averaging of the parameters at the common ion (In) interface layer, instead of abruptly ''switching'' from InAs to InP parameters at an arbitrary interface boundary of zero width.

In order to obtain the energies and the spatial distribution of the bound states, we use the Green's function formalism. The Green's functions of the barrier and the well materials, $G^{(b)}$ and $G^{(w)}$, are computed using efficient algorithms.[22–24] Then they are matched at the two interfaces, using the surface Green's function matching method,[25] in order to obtain the Green's function of the structure $G^{(s)}$. The energies and

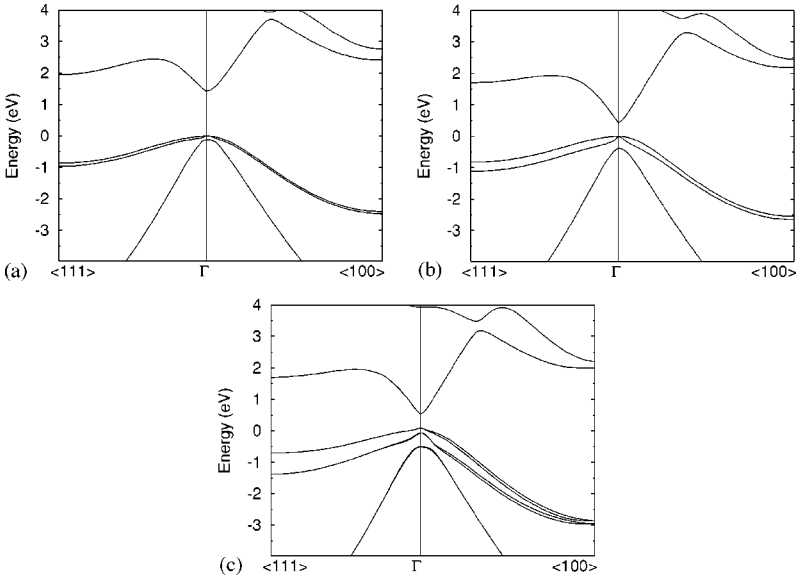

FIG. 1. Bulk band structures of InP (a), InAs (b), and InAs biaxially strained in the (001) plane to the bulk lattice constant of InP (c), calculated using the $sp^3d^5s^*$ tight-binding model.

the spatial distributions of the states are calculated from the local density of states (LDOS),

$$N(E,n) = -\frac{1}{\pi} \lim_{\epsilon \to +0} \mathrm{Im}\,\mathrm{Tr}[G^{(s)}_{n,n}(E + i\epsilon)], \qquad (2)$$

where E is the energy, n is the layer index, and $G^{(s)}_{n,n}$ is the diagonal element of the Green's function. We use a finite value of $\epsilon = 0.001$ eV, this is also the precision used to determine the energies of the bound states.

The effect of the interface grading on the transition energies is studied using the simple diffusion model of grading presented in Ref. 9. This model does not take into account lateral roughness and steplike interface structure, instead, it uses a concentration profile, averaged over the layer planes. This limitation is a consequence of the use of the virtual-crystal Hamiltonian and can be overcome by using more sophisticated methods like the supercell technique[10] or the coherent potential approximation[26] within the adopted Green's function approach. However, for the present work we favor the simplicity of the diffusion model and the virtual-crystal approximation. The diffusion length L_D is used as a parameter, giving the amount of grading present in the structure. Small values of L_D between 0 (abrupt interfaces) and 2 ML are used in order to model the interface grading. The strain in graded QWs is taken into account by assuming an in-plane lattice constant equal to that of bulk InP throughout the structure and calculating the interplane distances by using a linear approximation for the elasticity moduli of $InAs_xP_{1-x}$.

As usual in TB calculations, the heterojunction band offset is taken into account by adding a constant value to the diagonal tight-binding parameters (i.e., to the on-site orbital energies) of the well material, thus shifting its entire band structure with this value. However, the strain changes the energies of both the valence and the conduction band, and thus the value added to the TB parameters is not equal to the actual offset between the valence band maxima of the two materials. From here on, except where explicitly specified otherwise, by ''valence band offset'' (VBO) we shall mean the latter value, i.e., the ''strained'' VBO between InAs and InP. The constant added to the diagonal TB parameters of InAs (i.e., the ''unstrained'' valence band difference) may be obtained by adding to this value the position of the valence band maximum of strained InAs. In the $sp^3d^5s^*$ parameterization used in this work the latter is equal to 0.089 eV.

In the literature there is no clear indication for the effect of strain on the VBO. It has been argued on the basis of self-consistent TB calculations that the band offset in strained heterojunctions depends on strain.[27] Such a dependence may affect the bound states energies especially in structures with graded interfaces. On the other hand, it has been shown that the interdiffusion in systems with a common atom does not change the VBO.[28] Therefore we use the simple linear dependence of VBO on the alloy composition, resulting from the linearity of the virtual crystal approximation.

III. RESULTS AND DISCUSSION

A. Band offset

Various values for the VBO of the InAs/InP (001) heterojunction have been reported in the literature. A comprehensive review of the available experimental and theoretical results can be found in Ref. 16, where a recommended value of 0.35 eV is given for the unstrained heterojunction, corresponding to a strained VBO of 0.44 eV. The first-principles calculation of Wei and Zunger[29] gives a value of 0.42 eV, while the extrapolation from the experimental data on InAsP/InP quantum wells (VBO equal to 25% of the strained band gap difference[30]) gives a smaller VBO of 0.245 eV. A previous fit of the transition energies obtained by EFA calculations to experimental data on thin InAs/InP QWs suggests a value of 0.41 eV, while the same fit made with the TB method gives 0.47 eV (Ref. 31) (it is not clear though whether the latter two stand for strained or for unstrained VBO). The VBO is a property of the heterojunction, therefore, for QW widths in the monolayer range (i.e., when we have two het-

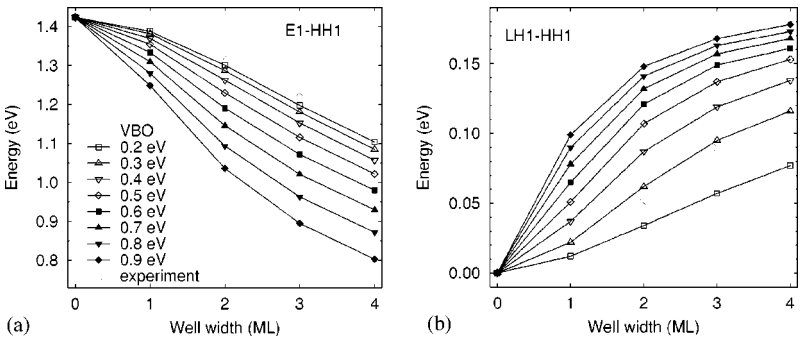

FIG. 2. Calculated E1–HH1 transition energies (a) and heavy hole–light hole splittings (b) in ultrathin InAs/InP QW for valence band offsets varying from 0.2 to 0.9 eV. Experimental values from Ref. 2 are also shown. Symbols represent the data points and the lines are drawn for guiding the eye.

erojunctions very close to each other) it is possible to have a VBO quite different than that for a wider QW. In order to take into account this possibility, while encompassing the entire range of values accepted for wider QWs, we vary the VBO from 0.2 to 0.9 eV. Later, when investigating particular features of the band structure for a fixed value of the VBO, we will use a composite value of 0.4 eV, obtained by averaging the cited results.

We have calculated the energies of the electronic states and the transition energies at the Γ point of the Brillouin zone for InAs/InP QWs from 1 to 4 monolayers (ML) wide. The obtained energies of the electron–heavy hole (E1–HH1) transition and of the heavy hole–light hole splitting are plotted in Fig. 2. When increasing the VBO, two main trends are observed: the E1–HH1 transition energy decreases and the HH1–LH1 splitting increases. The E1–HH1 transition energy is more sensitive to the VBO for greater VBOs due to the increased confinement of the HH1 state. The splitting, on the contrary, increases more rapidly for smaller VBOs. This is due mainly to the fact that the LH1 state is degenerate with the InP valence band at a VBO of 0.2 eV and emerges from the continuum at 0.3 eV, while the HH1 state is well confined in the entire range of VBOs considered. The E1 state in the 1 ML QW becomes degenerate with the InP conduction band at a VBO of 0.8 eV, for the other QWs its energy is a few meV below the continuum for a VBO of 0.9 eV.

We have also calculated the spatial distributions of the E1, HH1, and LH1 states. In the 1 ML well, we have obtained InP-localization of electrons only for VBO = 0.9 eV. The light-hole state is localized in the InP barrier only for VBO = 0.2 eV. For all other well widths and VBOs we observe InAs-confinement of the carrier wave functions. This finding contradicts a previous TB calculation,[5] made using the sp^3s^* model with an unstrained VBO of 0.42 eV (corresponding to a strained VBO of 0.51 eV), where InAs-confinement is found for heavy holes only. The experimentally observed heavy-hole and light-hole transition intensities,[2–4] however, also suggest type-I confinement of carriers in these structures, thus supporting our results.

The spatial distributions of the electron, heavy-hole and light-hole ground states, calculated for a VBO of 0.4 eV, are shown in Fig. 3. The fact that the spatial distributions are not symmetric with respect to the well center is due to the lack of inversion symmetry in the zinc-blende structure. As expected, in the 1 ML QW there is a weaker confinement of all carriers. This is very pronounced for the E1 and LH1 states, since they are closer to the respective barrier band edges, however it is clearly seen as well for the HH1 state. The E1 and LH1 states are more weakly localized in thinner wells, while for the heavy hole state this effect is significant only for the 1 ML QW. Therefore, we may expect the oscillator strength for the transitions in 1 ML QWs to be several times

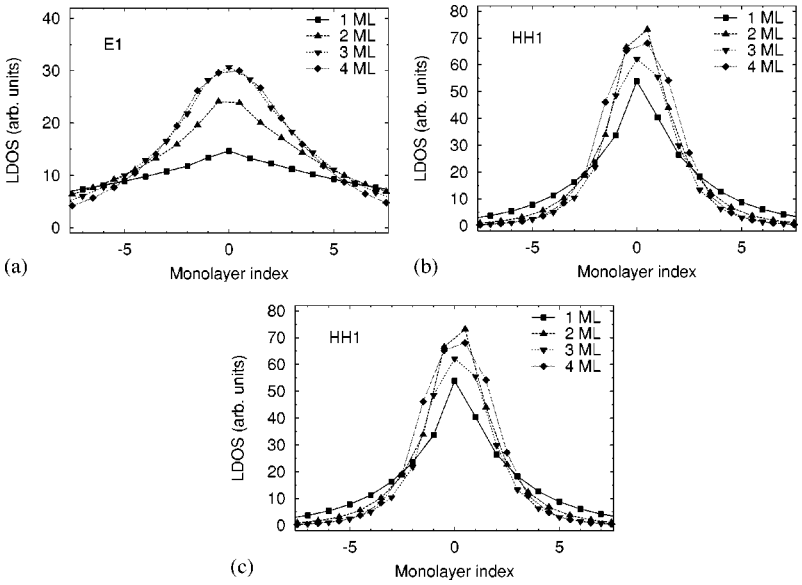

FIG. 3. Spatial distribution of the LDOS for the first electron (a), heavy-hole (b) and light-hole (c) states in InAs/InP QWs from 1 to 4 ML wide for VBO 0.4 eV. Monolayer index 0 represents the center of the QW.

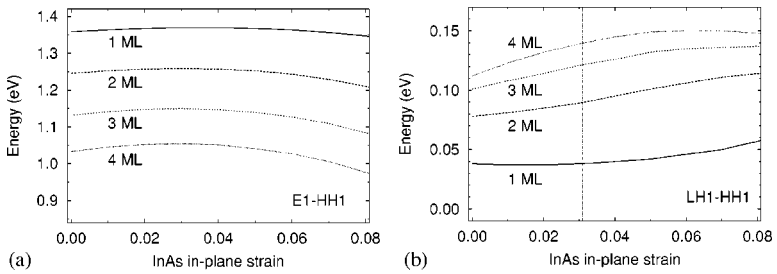

FIG. 4. Calculated dependence on strain of the E1–HH1 transition energies (a) and the heavy hole–light hole splittings (b) in ultrathin InAs/InP QW for VBO of 0.4 eV. The nominal strain of 3.1% is shown with a vertical line.

lower than in thicker wells. This may explain the fact that transitions from 1 ML QWs are not observed in the absorption spectra of samples with steplike interfaces,[2,3] where one may reasonably suggest the presence of regions with a thickness of 1 ML.

Our results are compared with the experimental data of Paki *et al.*[2] for the transition energies in 2 and 3 ML QWs. We neglect the exciton binding energies, since they are expected to be below the experimental error of 0.01 eV.[32] The experimental E1–HH1 and E1–LH1 transition energies (also shown in Fig. 2) are 1.23 and 1.32 eV in the 2 ML well and 1.32 and 1.37 eV in the 3 ML well, respectively. The heavy/light hole character of the transitions was confirmed by polarization-dependent measurements. It is seen in Fig. 2 that the E1–HH1 transition energies suggest a VBO below 0.2 eV. If this were the case, the LH1 state would be degenerate with the InP valence band, which would lead to a much weaker intensity of the light-hole transition with respect to the heavy-hole one. This, however, is not observed experimentally. On the other hand, the experimental HH–LH splitting is close to the calculated one for a VBO close to 0.3 eV. Therefore we can conclude that the experimental values cannot be explained by the simple model of a rectangular fully strained QW with abrupt interfaces.

B. Strain

One possible effect that can lead to the observed discrepancies between theoretical and experimental results is to have a strain value in the InAs layer different than the strain suggested by the difference between the bulk lattice constants of the two materials (3.1%). This can occur due to strain relaxation (smaller strain) or to accumulation of strain in the well layer (larger strain), which has been experimentally observed in ultrathin InAs layers in GaAs.[33] In order to estimate the effect of strain on the electronic states of thin QWs, we have calculated the dependence of the transition energies on strain, varying the strain in the InAs layer from 0 (completely relaxed layer) to 8%. The calculations are done keeping the same valence band difference between strained InAs and InP (0.4 eV) for each value of the strain. The results are presented in Fig. 4.

Our results show that the dependence of the E1–HH1 transition energy on strain is relatively weak. The transition energies are smaller for relaxed wells and have a maximum for approximately 3% strain (3.5% for 1 ML wells). This behavior generally follows the dependence of the band gap of InAs on strain. The variation of the transition energy for strain between 0 and 6% is relatively small—from 10 meV for the 1 ML well to 25 meV for the 4 ML well. These changes are greater for wider wells, which can be explained by recalling that strain shifts the potential in the well, and this has greater effect on the states energies in wider wells. Therefore, in wider wells strain is dominating, whereas for thinner wells the confinement has larger effect on the electronic states.

The heavy hole–light hole splitting, as a general rule, increases with increasing strain. This effect is, again, more pronounced for wider QWs, due to the reasons already discussed. The variation of the splitting energy is larger than that of the E1–HH1 transition, reaching 38 meV for the 4 ML QW. In our calculations the difference between the heavy-hole band edges of InP and strained InAs is kept constant independent on strain, i.e., the depth of the potential well for heavy holes remains constant and that for light holes decreases with strain. Therefore, the observed behavior is mainly due to the change in the HH–LH splitting of the bulk InAs valence bands due to strain. Because of the larger confinement energies in thinner QWs, however, the effective mass and band nonparabolicity changes with strain also play a significant role. This is well seen especially in the 1 ML QW, where a small decrease of the splitting energy is observed for strain between 0 and 1.8%—an effect, which is not seen in the dependence of the bulk band splitting on strain.

Our calculations for other values of the VBO show that the strain-induced shift of the transition energies is largest for VBOs between 0.3 and 0.4 eV. At this point the distribution of the band gap difference between the conduction and the valence bands makes the strain most efficient in changing the confinement energies of both electrons and holes. The exception of this trend is the E1–LH1 transition in the 1 ML QW, since in the latter the LH1 state is degenerate with the continuum for VBOs up to 3 meV and is therefore not affected by strain.

We compare the obtained strain dependence of the transition energies with the experimental data from Ref. 2. Assuming that some strain relaxation is present in the structures, one may obtain smaller HH–LH splitting energies, as suggested by the experiment. However strain effects cannot explain the fact that the experimental E1–HH1 transition energies are larger than the calculated ones, since both decreasing and increasing strain we obtain values smaller than the ones obtained for the nominal strain of 3.1%. Since our results show that the effect of strain is relatively small in ultrathin QWs, one may also suggest that the possible errors resulting from the nonsuitability of the macroscopic elasticity theory to predict the lattice constants for layers with monolayer-

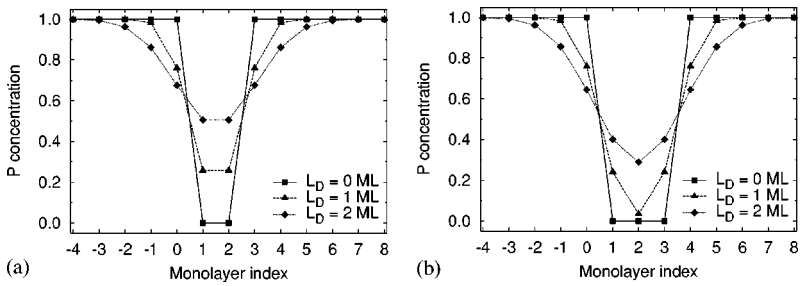

FIG. 5. Concentration profiles in 2 ML (a) and 3 ML (b) InAs/InP QWs for diffusion lengths L_D=0 (abrupt interfaces), 1, and 2 ML.

range thicknesses should be of the same order (20–30 meV) and could not account for the observed disagreement between theory and experiment.

C. Interface grading

It has been shown previously that very small amounts of interface grading in the AlGaAs/GaAs system have a significant effect on the bound states energies[9,10] and can dramatically influence features of the electronic structure such as the Γ–X mixing in superlattices.[11,12] There is experimental evidence that intermixing occurs during the growth of InAs/InP heterostructures.[13,14] Until now, however, only intentionally annealed QWs have been theoretically investigated.[15] Having shown that varying only the VBO and the strain it is impossible to obtain a satisfactory explanation of the experimental transition energies in ultrathin InAs/InP QWs, we further extend our model in order to take into account interface grading in these structures.

We investigate the effect of interface grading on the transition energies, assuming a diffusion model of the grading,[9] and using the diffusion length L_D as a parameter giving the amount of grading present in the structure. This model introduces a concentration profile, averaged over the layer planes, calculated as a solution of the diffusion equation for small values of the diffusion length. The calculated concentration profiles in the 2 and 3 ML QWs for values of L_D of 0, 1, and 2 ML are shown in Fig. 5. As expected for very thin QWs, the concentration profile changes significantly even for diffusion lengths as small as 1 ML. Still, for L_D=1 ML only the concentration of the layers adjacent to the interfaces changes noticeably, the change in the other layers being $<$3%. For L_D=2 ML the entire well profile is modified, and the concentration of P at the well center reaches 50% for the 2 ML QW and 29% for the 3 ML QW.

Figure 6 shows the results for the optical transition energies in 2 and 3 ML wide InAs/InP QWs with graded interfaces for a VBO of 0.4 eV. The transition energies of the graded QWs exhibit a blue shift with respect to the transitions in the rectangular QWs. This shift is slightly larger for the E1–HH1 transition, since the heavy hole energies are more sensitive to the changes of the well potential mainly due to the larger potential barrier. Thus, the interface grading also leads to a small decrease of the energy separation between the heavy hole and the light hole transition. The blue shift is larger in the 3 ML QW, and increases with the increase of the VBO. The maximum blue shift observed reaches 0.11 eV at a diffusion length of 2 ML for the E1–HH1 transition in the 3 ML QW at VBO of 0.6 eV. This behavior is similar to that reported by many authors for diffused QWs (see e.g., Ref. 34). The blue shift of the transitions in ultrathin wells, however, is much larger than the one in wider wells, because the same changes in the concentration profile occur at smaller diffusion lengths.

We have also calculated the spatial distributions of the bound states in ultrathin QWs with graded interfaces. A small decrease of the amplitude is observed with increasing L_D, however, in spite of the fact that the wells become significantly more shallow, the states remain well localized in the 2 and 3 ML QWs for the considered range of diffusion lengths. Therefore, the effect of interface grading should be manifested in the optical spectra only by changes in the transition energies.

In the figure are also shown the experimental transition energies for the E1–HH1 and E1–LH1 transitions in the 2 and 3 ML wells. It is seen that taking into account the interface grading we obtain an excellent agreement between the theoretical and the experimental results for L_D=1.8 ML. Our calculations for other values of the VBO show that a satisfactory agreement (within the experimental error of 0.01 eV) between the calculated and the experimental transition energies can be obtained for VBOs between 0.35 and 0.48 eV and diffusion lengths of 1.7–2.3 ML. These VBO values are within the range of acceptable values cited in the literature.

D. Well composition

Another possible effect of intermixing is to have a certain nonzero concentration of P in the well layer. In order to take

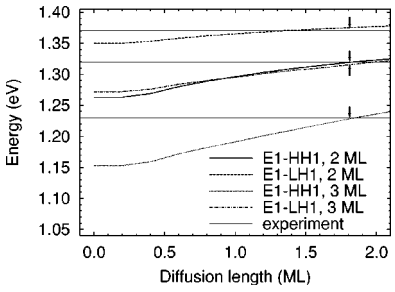

FIG. 6. Optical transition energies in 2 and 3 ML InAs/InP QWs with nonabrupt interfaces for VBO=0.4 eV. The experimental transition energies are shown with thin horizontal lines. The lower line at 1.23 eV corresponds to the E1–HH1 transition in the 3 ML well, the middle one at 1.32 eV represents the E1–LH1 in the 3 ML QW and the E1–HH1 in the 2 ML QW, and the line at 1.37 eV corresponds to the E1–LH1 transition in the 2 ML QW. The results giving best fit to experiment are shown with arrows (L_D=1.8 ML).

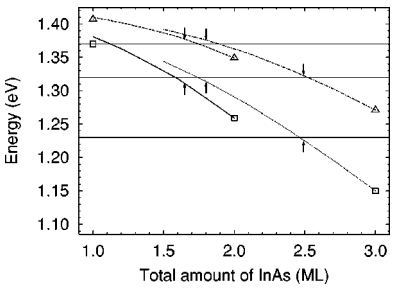

FIG. 7. Transition energies in rectangular 2 and 3 ML $InAs_xP_{1-x}$/InP QWs with varying composition of the well material and a VBO of 0.4 eV. E1−HH1 and E1−LH1 transition energies are plotted with the solid and dashed line in the 2 ML well, and with the dotted and dashed−dotted line in the 3 ML well. The energies of 1, 2, and 3 ML InAs/InP QWs ($x=1$) are shown with squares and triangles for heavy and light-hole transitions, respectively. The experimental transition energies are shown with horizontal lines. The values giving the best fit to the experiment are shown with arrows.

into account this possibility, we consider rectangular $InAs_xP_{1-x}$/InP QWs. The calculated transition energies in 2 and 3 ML rectangular $InAs_xP_{1-x}$/InP QWs for a VBO of 0.4 ML are shown in Fig. 7. The dependencies are plotted versus the total amount of InAs in the structure, which can be expressed in units of ML by multiplying the InAs concentration x in the well by the well width in ML. We note that the $InAs_xP_{1-x}$/InP QWs considered here differ from the InAs/InP QWs considered in the previous sections as they may contain a total amount of InAs *not equal to an integer number of monolayers*.

It is seen from the figure that the effects of decreasing the As concentration x in the QW are similar to those of increased interface grading: (i) the transition energies increase and (ii) the heavy hole−light hole splitting decreases. The transition energies of wider wells are higher than those in more narrow wells with the same amount of InAs, and this effect is more pronounced for the heavy-hole transition. The differences between the transition energies in 2 and 3 ML QWs, both containing 2 ML of InAs, are 32 meV and 14 meV for the heavy- and light-hole transitions, respectively.

Comparing the calculations with the experimental results (also shown in Fig. 7) we see that the first pair of transitions, attributed to the 2 ML QW (E1−HH1=1.27 eV, E1−LH1 =1.32 eV), can be satisfactory explained by assuming either a 2 ML QW with $x=0.83$ (corresponding to a total amount of InAs 1.65 ML), or a 3 ML QW with $x=0.6$ (total amount of InAs 1.8 ML). For the other pair of transition energies (E1−HH1=1.32 eV, E1−LH1=1.37 eV), attributed to the 3 ML QW, we obtain an excellent agreement for a 3 ML QW with $x=0.83$ (corresponding to 2.5 ML InAs).

The thickness of the QWs in Ref. 2 is measured using high-resolution x-ray diffraction (HRXRD). These measurements are sensitive to the average amount of the well material present in the sample. In samples such as the ones described in Ref. 2 the presence of QW regions (islands) of two different widths is suggested by the optical data. Therefore, the average amount of well material in the sample (hence, the HRXRD data) depend not only on the composition, but also on the relative area of each region as a fraction of the whole area of the sample. Thus, it is impossible to obtain a precise estimate of the width and composition of each QW based only on the HRXRD results. However, assuming the presence of 2 and 3 ML QW regions in the samples due to a monolayer step at the interface, we obtain a good agreement with the experiment for both QWs at a composition of the well material $InAs_{0.83}P_{0.17}$. We have obtained the same result also for a VBO of 0.3 eV at an As concentration $x=87.5\%$.

When one investigates InAs/InP QWs with perfectly abrupt interfaces by means of an atomistic method such as TB, the model is restricted to considering only QWs containing an integer number of InAs monolayers due to its discrete nature. However, taking into account the interface grading and considering concentration profiles such as the ones shown in Fig. 5, it is easily seen that this restriction no longer has physical grounds. One may suggest that during the growth of ultrathin QWs both effects occur; the interfaces are non-abrupt due to atomic-scale roughness and component interdiffusion, and they contain an arbitrary (not equal to an integer number of monolayers) amount of the well material. Since both the increasing of the interface grading and the decreasing of the amount of InAs in the QW have the same influence on the transition energies, one needs more precise data on the sample structure and composition in order to make a comparison between theoretical and experimental results. Good candidates for such a study are samples in which the well thickness is uniform throughout the area of the sample (see e.g., Ref. 4), because the total amount of the well material can be unambiguously obtained by HRXRD measurements.

IV. CONCLUSION

We have calculated the optical transition energies in strained ultrathin InAs/InP (001) QWs using the semiempirical $sp^3d^5s^*$ tight-binding method, the virtual crystal approximation, and the surface Green's function matching technique. QWs from 1 to 4 ML wide are considered. The effect of a number of factors on the transition energies is systematically investigated: valence band offset, strain, interface grading, and well composition. We start with the simple model of a rectangular fully strained QW. Then we investigate the dependence of the transition energies on strain in order to take into account the possibility to have InAs strain values different than 3.1% (the difference in the bulk lattice constants of the two materials) due to the very small thickness of the InAs layer. Further, we extend our treatment in order to include intermixing effects by considering (i) graded interfaces with a diffusion concentration profile, and (ii) QWs with abrupt interfaces and varying composition of the well material. The effect of strain on the transition energies is found to be small for thin wells, where the confinement is very strong and therefore dominating. The effect of intermixing is, on the contrary, more pronounced in thinner wells because they are sensitive to very small changes in the interface potential. Our results show that the shift of the transition energies obtained by either introducing graded interfaces or changing the well composition is significant and cannot be

neglected in theoretical calculations, especially knowing that intermixing may occur during the growth of InAs/InP heterostructures.[13,14]

Comparing our calculated results with experimental data, we show that the experimental transition energies cannot be accounted for by a simple model of a fully strained rectangular QW. The effects of strain different than 3.1% also cannot explain the experimental observations. Considering QWs with nonabrupt interfaces we have shown that a reasonable agreement with the experimental results is obtained for VBOs between 0.35 and 0.48 eV, which is consistent with the majority of results on the InAs/InP heterojunction band offset,[16] and for diffusion lengths of 1.8–2.3 ML. A good agreement with the experimental results can be obtained also by assuming rectangular $InAs_xP_{1-x}/InP$ QWs with a concentration of As in the well $x=0.83$. Thus, the comparison of theory with experiment also shows that taking into account the intermixing effects is important in order to obtain an accurate description of the electronic properties of ultrathin quantum wells.

ACKNOWLEDGMENTS

The authors gratefully acknowledge the financial support of the Natural Sciences and Engineering Research Council of Canada during the course of this research. P.D. also acknowledges support from the Canada Research Chair Program.

*Electronic address: nshtinkov@polymtl.ca

[1] R. A. Masut, C. A. Tran, M. Beaudoin, and R. Leonelli, Proc. SPIE **2398**, 116 (1995).
[2] P. Paki, R. Leonelli, L. Isnard, and R. A. Masut, Appl. Phys. Lett. **74**, 1445 (1999).
[3] P. Paki, R. Leonelli, L. Isnard, and R. A. Masut, J. Vac. Sci. Technol. A **18**, 956 (2000).
[4] D. Frankland, R. A. Masut, and R. Leonelli, J. Vac. Sci. Technol. A **20**, 1132 (2002).
[5] V. Albe and L. J. Lewis, Physica B **301**, 233 (2001).
[6] M. Di Ventra and K. A. Mäder, Phys. Rev. B **55**, 13 148 (1997).
[7] R. C. Iotti, L. C. Andreani, and M. Di Ventra, Phys. Rev. B **57**, R15 072 (1998).
[8] Y. Foulon and C. Priester, Phys. Rev. B **44**, 5889 (1991).
[9] N. Shtinkov, V. Donchev, K. Germanova, and H. Kolev, Semicond. Sci. Technol. **15**, 946 (2000).
[10] B. Koiller, A. S. Martins, and H. Chacham, Appl. Phys. Lett. **69**, 2423 (1996).
[11] N. Shtinkov, S. Vlaev, and V. Donchev, Phys. Status Solidi B **221**, R9 (2000).
[12] J. G. Menchero, B. Koiller, and R. B. Capaz, Phys. Rev. Lett. **83**, 2034 (1999).
[13] J. Brault, M. Gendry, G. Grenet, G. Hollinger, Y. Desières, and T. Benyattou, Appl. Phys. Lett. **73**, 2932 (1998).
[14] L. G. Quagliano, B. Jusserand, and D. Orani, Phys. Rev. B **56**, 4919 (1997).
[15] J. M. Sallese, S. Taylor, H. J. Bühlmann, J. F. Carlin, A. Rudra, R. Houdré, and M. Illegems, Appl. Phys. Lett. **65**, 341 (1994).
[16] I. Vurgaftman, J. R. Meyer, and L. R. Ram-Mohan, J. Appl. Phys. **89**, 5815 (2001).
[17] P. Vogl, H. P. Hjalmarson, and J. D. Dow, J. Phys. Chem. Solids **44**, 365 (1983).
[18] C. Priester, G. Allan, and M. Lannoo, Phys. Rev. B **37**, 8519 (1988).
[19] J.-M. Jancu, R. Scholz, F. Beltram, and F. Bassani, Phys. Rev. B **57**, 6493 (1998).
[20] T. B. Boykin, G. Klimeck, R. C. Bowen, and R. Lake, Phys. Rev. B **56**, 4102 (1997).
[21] W. A. Harrison, *Electronic Structure and the Properties of Solids* (Freeman, San Francisco, 1980).
[22] M. P. López-Sancho, J. M. López-Sancho, and J. Rubio, J. Phys. F: Met. Phys. **14**, 1205 (1984).
[23] M. P. López-Sancho, J. M. López-Sancho, and J. Rubio, J. Phys. F: Met. Phys. **15**, 851 (1985).
[24] S. Vlaev, V. R. Velasco, and F. García-Moliner, Phys. Rev. B **49**, 11 222 (1994).
[25] F. García-Moliner and V. R. Velasco, *Theory of Single and Multiple Interfaces* (World Scientific, Singapore, 1992).
[26] K. M. Hong, P. C. K. Kwok, and P. C. Chui, Solid State Commun. **107**, 483 (1998).
[27] C. Priester, G. Allan, and M. Lannoo, Phys. Rev. B **38**, 9870 (1988).
[28] Y. Foulon and C. Priester, Phys. Rev. B **45**, 6259 (1992).
[29] S.-H. Wei and A. Zunger, Appl. Phys. Lett. **72**, 2011 (1998).
[30] M. Beaudoin, A. Bensaada, R. Leonelli, P. Desjardins, R. A. Masut, L. Isnard, A. Chennouf, and G. L'Espérance, Phys. Rev. B **53**, 1990 (1996).
[31] A. Bitz, C. Jordan, M. Di Ventra, K. A. Mäder, L. C. Andreani, J. F. Carlin, A. Rudra, and J. L. Staehli, Nuovo Cimento D **17**, 1367 (1995).
[32] M. Sugawara, N. Okazaki, T. Fujii, and S. Yamazaki, Phys. Rev. B **48**, 8102 (1993).
[33] O. Brandt, K. Ploog, R. Bierwolf, and M. Hohenstein, Phys. Rev. Lett. **68**, 1339 (1992).
[34] S. J. Vlaev and D. A. Contreras-Solorio, J. Appl. Phys. **82**, 3853 (1998).